

Conditional Expectation Network for SHAP

Ronald Richman* Mario V. Wüthrich†

Version of July 21, 2023

Abstract

A very popular model-agnostic technique for explaining predictive models is the **SH**apley **A**dditive **eX**planation (SHAP). The two most popular versions of SHAP are a conditional expectation version and an unconditional expectation version (the latter is also known as interventional SHAP). Except for tree-based methods, usually the unconditional version is used (for computational reasons). We provide a (surrogate) neural network approach which allows us to efficiently calculate the conditional version for both neural networks and other regression models, and which properly considers the dependence structure in the feature components. This proposal is also useful to provide `drop1` and `anova` analyses in complex regression models which are similar to their generalized linear model (GLM) counterparts, and we provide a partial dependence plot (PDP) counterpart that considers the right dependence structure in the feature components.

Keywords. Shapley value, SHAP, conditional SHAP, unconditional SHAP, interventional SHAP, anova, drop1, analysis-of-deviance, least squares Monte Carlo, partial dependence plot, PDP, explainability, XAI.

1 Introduction

We start by formally introducing the problem studied in this paper. We consider a random tuple (Y, \mathbf{X}) with Y describing a real-valued response variable that is supported by features $\mathbf{X} = (X_1, \dots, X_q)^\top$ taking values in a feature space $\mathcal{X} \subseteq \mathbb{R}^q$. We use these features to build a regression model

$$\mu : \mathcal{X} \rightarrow \mathbb{R}, \quad \mathbf{x} \mapsto \mu(\mathbf{x}), \quad (1.1)$$

that serves at predicting the response variable Y , e.g., we can use the conditional expectation regression function defined by

$$\mathbf{x} \mapsto \mu(\mathbf{x}) = \mathbb{E}[Y | \mathbf{X} = \mathbf{x}].$$

The problem that we solve in this paper is the computation of the conditionally expected regression function (1.1), if only a subset of the feature components of $\mathbf{X} = (X_1, \dots, X_q)^\top$ is available.

*Old Mutual Insure and University of the Witwatersrand, Johannesburg, South Africa; ronaldrichman@gmail.com

†RiskLab, Department of Mathematics, ETH Zurich, mario.wuethrich@math.ethz.ch

E.g., if only the first two components $(X_1, X_2) = (x_1, x_2)$ of \mathbf{X} are observed, we would like to compute the conditional expectation

$$\mathbb{E}[\mu(\mathbf{X}) | X_1 = x_1, X_2 = x_2], \quad (1.2)$$

this is further motivated in Example 2.1, below. Such conditional expectations (1.2) are of interest in many practical problems, e.g., they enter the **SH**apley **A**dditive **eX**planation (SHAP) of Lundberg–Lee [24], see also Aas et al. [1], they are of interest in discrimination-free insurance pricing, see Lindholm et al. [21], and they are also useful in a variable importance analysis, similar to the **anova** (analysis-of-variance/analysis-of-deviance) and the **drop1** analyses for generalized linear models (GLMs) in the R statistical software [29], see also Section 2.3.2 in McCullagh–Nelder [28]. Moreover, it is known that the partial dependence plot (PDP) of Friedman [10] and Zhao–Hastie [37] for marginal explanation cannot correctly reflect the dependence structure in the features \mathbf{X} . Below, we provide an alternative proposal, called marginal conditional expectation plot (MCEP), that mitigates this deficiency.

The main difficulty in efficiently evaluating (1.2) is that it has a similar computational complexity as nested simulations, if one wants to calculate these conditional expectations (1.2) with Monte Carlo simulations for all possible values (x_1, x_2) . That is, we need to simulate for *all* values (x_1, x_2) the random vector (X_3, \dots, X_q) conditionally, given $(X_1, X_2) = (x_1, x_2)$. Such nested simulations are computationally expensive, and things become even more involved if we need to calculate these conditional expectations for *all* possible subsets of the components of \mathbf{X} , e.g., when performing a SHAP analysis. A further difficulty is that these simulations can only be done by bootstrapping if the true probability law π of \mathbf{X} is unknown, i.e., if we have to rely on an i.i.d. sample $(\mathbf{X}_i)_{i=1}^n$ of $\mathbf{X} \sim \pi$. In that case sparsity of observations in different parts of the feature space \mathcal{X} poses another issue, and this issue becomes more serious for higher dimensional features \mathcal{X} .

In financial mathematics, a similar problem occurs when evaluating American options. Carriere [5], Longstaff–Schwartz [22] and Tsitsiklis–Van Roy [35] have proposed to map the (inner) nested valuation problem to a suitable class of basis functions; this is also known as least squares Monte Carlo (LSMC). Basically, this means that (1.2) should be expressed as a new regression function in the variables (x_1, x_2) , and this new (inner) regression function still needs to be determined. Benefiting from the huge modeling flexibility of neural networks (universal approximation property), it has been proposed to use a neural network as this new inner regression function; see, e.g., Cheridito et al. [7], Krah et al. [18] or Jonen et al. [17]. These proposals have been made for a fixed set of observable components of \mathbf{X} .

Our main contribution extends the set-up of Cheridito et al. [7] to simultaneously model the conditional expectations of all possible subsets of observable components of \mathbf{X} . This allows us to develop a fast algorithm for estimating conditional SHAP, based on a surrogate neural network; this proposal works both for neural networks and other predictive machine learning algorithms. We discuss the necessary variable masking used, and we propose a specific fitting procedure so that the extreme cases about the full knowledge of \mathbf{X} and about the null model (not knowing \mathbf{X}) are correctly calibrated. Furthermore, we present applications of this approach to model-agnostic variable importance tools, such as an **anova** or a **drop1** analysis, similar to GLMs, MCEPs similar to PDPs, and a global conditional SHAP decomposition of the generalization loss.

Organization. In the next section, we introduce the surrogate neural network for conditional expectation estimation, and we discuss the specific fitting procedure so that the extreme cases of full knowledge and of zero knowledge are properly calibrated. In Section 3, we apply these conditional expectations to analyses variable importance in predictive models. For this we introduce an **anova** analysis and a **drop1** analysis that are similar to their GLM counterparts, see Section 3.2. In Section 3.3, we introduce the marginal conditional expectation plot (MCEP) as a conditional expectation counterpart of the partial dependence plot (PDP) that properly considers the dependence structure in the features. In Section 4, we discuss the application of our proposal to efficiently calculate the conditional SHAP. On the one hand, we consider the individual (local) mean decomposition, and on the other hand a global fair SHAP score decomposition for variable importance. Finally, Section 5 concludes.

2 Conditional expectation network

We begin from a given regression function $\mathbf{x} \mapsto \mu(\mathbf{x})$, which maps the feature values $\mathbf{x} = (x_1, \dots, x_q)^\top \in \mathcal{X} \subseteq \mathbb{R}^q$ to real-valued output values $\mu(\mathbf{x}) \in \mathbb{R}$; we assume that this regression function μ is given. In our example below, this regression function has been constructed within a fixed (given) network architecture based on an i.i.d. sample $(Y_i, \mathbf{x}_i)_{i=1}^n$. However, this is not an essential point in our proposal. The following methodology can be applied to any other regression model, such as gradient boosting trees, nonetheless, if the regression function $\mathbf{x} \mapsto \mu(\mathbf{x})$ comes from a neural network, it will speed up the following (network) model fitting procedure, because the gradient descent algorithm can be initialized with exactly the network weights as used in the (first) regression function μ .

Assume that $\mathbf{X} \sim \pi$ denotes the random selection of a feature value $\mathbf{X} = \mathbf{x} \in \mathcal{X}$. Select a subset $\mathcal{C} \subseteq \mathcal{Q} := \{1, \dots, q\}$ of the feature component indices. We generically write $\mathbf{X}_{\mathcal{C}} = (X_j)_{j \in \mathcal{C}}$ for selecting the components of \mathbf{X} with indices $j \in \mathcal{C}$. Our goal is to calculate the conditional expectations

$$\mu_{\mathcal{C}}(\mathbf{x}) := \mathbb{E}[\mu(\mathbf{X}) | \mathbf{X}_{\mathcal{C}} = \mathbf{x}_{\mathcal{C}}], \quad (2.1)$$

with the two extreme cases $\mathcal{C} = \emptyset$ and $\mathcal{C} = \mathcal{Q}$ given by

$$\mu_{\emptyset} := \mu_{\emptyset}(\mathbf{x}) = \mathbb{E}[\mu(\mathbf{X})] \quad \text{and} \quad \mu_{\mathcal{Q}}(\mathbf{x}) = \mathbb{E}[\mu(\mathbf{X}) | \mathbf{X} = \mathbf{x}]. \quad (2.2)$$

The former is called the *null model* and the latter is the *full model*. In general, the conditional expectation $\mu_{\mathcal{C}}(\mathbf{x})$ cannot easily be calculated because in regression function $\mathbf{x} \mapsto \mu(\mathbf{x})$, we cannot simply “turn off” the components of \mathbf{x} that are not in \mathcal{C} .

Example 2.1 Assume Y is an integrable random variable and that the full model is given by the conditional expectation regression function

$$\mathbf{x} \mapsto \mu(\mathbf{x}) = \mathbb{E}[Y | \mathbf{X} = \mathbf{x}]. \quad (2.3)$$

If, for some reason, only the components $\mathbf{X}_{\mathcal{C}}$ of \mathbf{X} , $\mathcal{C} \subset \mathcal{Q}$, have been observed, then we can only build a regression model

$$\mathbf{x}_{\mathcal{C}} = (x_j)_{j \in \mathcal{C}} \mapsto \mathbb{E}[Y | \mathbf{X}_{\mathcal{C}} = \mathbf{x}_{\mathcal{C}}] = \mathbb{E}[\mu(\mathbf{X}) | \mathbf{X}_{\mathcal{C}} = \mathbf{x}_{\mathcal{C}}] = \mu_{\mathcal{C}}(\mathbf{x}),$$

where we have used the tower property of conditional expectations. Thus, the conditional expectation (2.1) naturally arises under partial information. Note that the full model $\mu = \mu_{\mathcal{Q}}$ given in (2.3) dominates in convex order any other regression function $\mu_{\mathcal{C}}$, $\mathcal{C} \subset \mathcal{Q}$, i.e., it has a higher resolution than any other conditional expectation regression function; see also Theorem 2.27 in Gneiting–Resin [11] for the resolution (discrimination) of a regression model. ■

We assume that all considered random variables are square integrable. This implies that we can work on a Hilbert space. We then receive the conditional expectation $\mu_{\mathcal{C}}(\mathbf{X})$ as the orthogonal projection of $\mu(\mathbf{X})$ onto the subspace $\sigma(\mu_{\mathcal{C}}(\mathbf{X}))$ generated by random variable $\mu_{\mathcal{C}}(\mathbf{X})$ in this Hilbert space. That is, the conditional expectation is the measurable function $\mathbf{x}_{\mathcal{C}} = (x_j)_{j \in \mathcal{C}} \mapsto \mu_{\mathcal{C}}(\mathbf{x})$ that minimizes the mean squared distance

$$\mathbb{E} \left[(\mu(\mathbf{X}) - \mu_{\mathcal{C}}(\mathbf{X}))^2 \right] \stackrel{!}{=} \min.$$

Among all $\mathbf{x}_{\mathcal{C}}$ -measurable functions, this conditional expectation is obtained by the solution of

$$\mu_{\mathcal{C}}(\mathbf{x}) = \arg \min_{\hat{\mu}} \mathbb{E} \left[(\mu(\mathbf{X}) - \hat{\mu})^2 \mid \mathbf{X}_{\mathcal{C}} = \mathbf{x}_{\mathcal{C}} \right], \quad (2.4)$$

for π -a.e. $\mathbf{x}_{\mathcal{C}}$. The idea now is to approximate the functions $\mathbf{x}_{\mathcal{C}} \mapsto \mu_{\mathcal{C}}(\mathbf{x})$ simultaneously for all subsets $\mathcal{C} \subseteq \mathcal{Q}$ by a neural network

$$\mathbf{x} \mapsto \text{NN}_{\vartheta}(\mathbf{x}), \quad (2.5)$$

where NN_{ϑ} denotes a neural network of a fixed architecture with network weights (parameter) ϑ . There are two important points to be discussed:

- (1) The neural network (2.5) considers all components of input \mathbf{x} . In order that this network can approximate $\mu_{\mathcal{C}}(\mathbf{x})$, we need to mask all components in $\mathbf{x} = (x_1, \dots, x_q)^{\top}$ which are not contained in \mathcal{C} . Choose a mask value $\mathbf{m} = (m_1, \dots, m_q)^{\top} \in \mathbb{R}^q$, the specific choice is going to be discussed below; for the moment, it should just be a sort of “neutral value”.

We set

$$\mathbf{x}_{\mathcal{C}}^{(\mathbf{m})} := (m_1 + (x_1 - m_1)\mathbb{1}_{\{1 \in \mathcal{C}\}}, \dots, m_q + (x_q - m_q)\mathbb{1}_{\{q \in \mathcal{C}\}})^{\top}. \quad (2.6)$$

We then try to find an optimal network parameter ϑ such that $\text{NN}_{\vartheta}(\mathbf{x}_{\mathcal{C}}^{(\mathbf{m})})$ is a good approximation to $\mu_{\mathcal{C}}(\mathbf{x})$ for all features $\mathbf{x} \in \mathcal{X}$ and all subsets $\mathcal{C} \subseteq \mathcal{Q}$.

- (2) In our applications, we explore an empirical version of (2.4) to find the optimal network parameter ϑ . Assume we have observed features $(\mathbf{x}_i)_{i=1}^n$. Then, we solve

$$\hat{\vartheta} = \arg \min_{\vartheta} \frac{1}{3n} \sum_{l=1}^{3n} \left(\tilde{\mu}(\mathbf{x}_l^{[3]}) - \text{NN}_{\vartheta}(\mathbf{x}_l^{[3]}) \right)^2, \quad (2.7)$$

where, to both calibrate the network and meet the logical constraints of the full and the null model, we triplicate the observed features $(\mathbf{x}_i)_{i=1}^n$ as follows:

- (a) For $1 \leq l \leq n$, we set $\mathbf{x}_l^{[3]} = \mathbf{x}_l$ and $\tilde{\mu}(\mathbf{x}_l^{[3]}) = \mu(\mathbf{x}_l)$. These instances are used to ensure that we can replicate the full model, see (2.2).
- (b) For $n + 1 \leq l \leq 2n$, we set $\mathbf{x}_l^{[3]} = \mathbf{m}$ and $\tilde{\mu}(\mathbf{x}_l^{[3]}) = \mu_0$. These instances are used to ensure that we can replicate the null model, see (2.2). If μ_0 is not available we just take the empirical mean of $(\mu(\mathbf{x}_i))_{i=1}^n$ as its estimate.

- (c) For $2n + 1 \leq l \leq 3n$, we set $\mathbf{x}_l^{[3]} = \mathbf{x}_{l-2n, \mathcal{C}_l}^{(\mathbf{m})}$, see (2.6), and $\tilde{\mu}(\mathbf{x}_l^{[3]}) = \mu(\mathbf{x}_l)$, where the sets $\mathcal{C}_l \subseteq \mathcal{Q}$ are chosen randomly and independently such that they mask independently of all other components each component $j \in \mathcal{Q}$ with probability $1/2$.

Remarks 2.2 • We use the above cases (a) and (b) with indices $1 \leq l \leq 2n$ to ensure that the extreme cases (2.2), the null model μ_0 and the full model $\mu(\mathbf{x})$, can be approximated by the estimated neural network $\text{NN}_{\hat{\theta}}$. These two cases serve as calibration of the conditional expectations.

- The above case (c) with indices $2n + 1 \leq l \leq 3n$ models the conditional expectations (2.1), where the input data $\mathbf{x}_l^{[3]} = \mathbf{x}_{l-2n, \mathcal{C}_l}^{(\mathbf{m})}$ has randomly masked components m_j with $j \notin \mathcal{C}_l$, and it tries to approximate the full model as well as possible.
- In relation to the previous item, there is some connection to masked auto-encoders which randomly mask part of the input images, which are then reconstructed by the auto-encoders; see He et al. [14]. These masked auto-encoders are used for denoising, in our application this denoising can be interpreted as taking conditional expectations.
- The network in (2.7) is fitted with gradient descent, and if the first model $\mu(\mathbf{x})$ is also a network with the same architecture, we propose to initialize gradient descent optimization of (2.7) precisely with the network weights of the first model $\mu(\mathbf{x})$.
- For stochastic gradient descent, one should randomize to order of the indices $1 \leq l \leq 3n$ in (2.7), so that all random mini-batches have instances of all three kinds.
- We mask the input data $\mathbf{x}_{l-2n, \mathcal{C}_l}^{(\mathbf{m})}$, see item (c) above, i.e., every component of \mathbf{x}_l is masked independently from the others with probability $1/2$. This precisely corresponds to selecting each subset $\mathcal{C} \subseteq \mathcal{Q}$ in the SHAP computation (4.3) with equal probability, which results in 2^q subsets of equal probability. Alternatively, equivalently, one could also use a drop-out layer after the input with a drop-out probability of $1/2$. However, this drop-out approach provides different difficulties. Drop-out uses the mask value 0, and it cannot easily calibrate the extreme cases of the null model and the full model. Moreover, drop-out may be more difficult in implementation if one uses entity embeddings for categorical feature components (because these act simultaneously on multiple embedding weights). Our example below will use entity embeddings for categorical feature components.

There remains the discussion of the mask value $\mathbf{m} \in \mathbb{R}^q$ in (2.6). We start with the case where \mathbf{x} only has continuous components. In that case, it may happen that there is a feature \mathbf{x} that takes the same value as the mask $\mathbf{m} \in \mathbb{R}^q$, i.e., $\mathbf{x} = \mathbf{m}$. In the fully masked case we should obtain the null model

$$\mu_0 = \mu_\emptyset(\mathbf{x}) \stackrel{!}{=} \text{NN}_{\hat{\theta}}(\mathbf{m}),$$

i.e., the estimated network $\text{NN}_{\hat{\theta}}$ can perfectly replicate the null model if the feature $\mathbf{X} = \mathbf{m}$ is fully masked. At the same time for the (non-masked) feature value $\mathbf{x} = \mathbf{m}$, we should obtain in the full model

$$\mu(\mathbf{x}) = \mu(\mathbf{m}) = \mu_{\mathcal{Q}}(\mathbf{m}) \stackrel{!}{=} \text{NN}_{\hat{\theta}}(\mathbf{m}).$$

These two requirements do not stay in conflict, if we choose the mask value $\mathbf{m} \in \mathbb{R}^q$ such that

$$\mu(\mathbf{m}) = \mu_0, \tag{2.8}$$

i.e., we choose the mask value \mathbf{m} such that the full model has the same prediction in $\mathbf{x} = \mathbf{m}$ as the null model (not considering any features).

In practical neural network applications, we typically normalize the continuous feature components of \mathbf{x} to be centered and have unit variance. This is done to ensure efficient gradient descent fitting. As a consequence, the continuous feature components of \mathbf{x} fluctuate around zero. To select the mask value \mathbf{m} we proceed as follows in our application below. We choose a small tolerance level $\delta > 0$ (we choose $\delta = 0.1\%$ in our application), and we select the mask value $\mathbf{m} \in \mathbb{R}^q$ as close as possible to the origin among all observed features $(\mathbf{x}_i)_{i=1}^n$ whose regression value $\mu(\mathbf{x}_i)$ differs less than δ from the null model μ_0 . That is,

$$\mathbf{m} = \underset{\mathbf{x}_i: |\mu(\mathbf{x}_i) - \mu_0| < \delta}{\arg \min} \|\mathbf{x}_i\|, \quad (2.9)$$

where $\|\cdot\|$ is the Euclidean norm. Having a mask value close to the origin ensures that the mask is in the main body of the (normalized) distribution of the continuous features.

Remarks 2.3 • This proposal (2.9) has some similarity to the Baseline SHAP presented in Sundararajan–Najmi [33], where the masked values are set to a baseline feature value \mathbf{x}' . However, the crucial difference is that we do not explicitly use this baseline feature value in our calculation because we perform a full conditional expectation in (2.1), but we only use the mask to indicate the network which variables have not been observed. In some sense, this is equivalent to “turning off” some input components as in drop-out layers, except that our mask value \mathbf{m} is chosen such that in the fully masked (turned off) case, we rediscover the null model.

- The crucial property of the choice of the mask \mathbf{m} is that it can both reflect the null model μ_0 and the expected value $\mu(\mathbf{m})$ in the mask $\mathbf{x} = \mathbf{m}$ in the full model, see (2.8). A mask choice close to zero (2.9) has another nice interpretation, namely, that values close to zero do not have any big effects given the affine transformations in neural network layers.
- Remark that the mask choice (2.9) has provided better models than choosing a (remote) mask value, e.g., $\mathbf{m} = (2, \dots, 2)^\top$, in the case of normalized features \mathbf{x} . Theoretically, there should not be any difference between this choice and choice (2.9) for large neural networks. However, this latter choice has turned out to be more difficult in gradient descent fitting, therefore, we prefer (2.9). Intuitively, a remote mask value will mean in this set-up that the null model is not discovered within the full model, but it is rather modeled separately beside the full model.

For the implementation of categorical feature components we use the method of entity embedding. Assume that X_j is a categorical variable that takes values in the (nominal) set $\mathcal{A}_j = \{a_1, \dots, a_K\}$, i.e., X_j takes K different levels $(a_k)_{k=1}^K$. For entity embedding, one chooses an embedding dimension $b \in \mathbb{N}$, and then each level $a_k \in \mathcal{A}_j$ is assigned an embedding weight $\mathbf{b}_k \in \mathbb{R}^b$. That is, we consider the embedding map

$$\mathbf{e} : \mathcal{A}_j \rightarrow \mathbb{R}^b, \quad X_j = a_k \mapsto \mathbf{e}(X_j) = \mathbf{b}_k;$$

we refer to Brébisson et al. [3], Guo–Berkhahn [13], Richman [30, 31] and Delong–Kozak [8]. The embedding $\mathbf{e}(X_j) \in \mathbb{R}^b$ is then concatenated with the continuous components of \mathbf{X} , and this

concatenation is used as input to the network. Entity embedding adds another Kb parameters $[\mathbf{b}_1, \dots, \mathbf{b}_K] \in \mathbb{R}^{b \times K}$ to the fitting procedure and these embedding parameters are also learned during gradient descent network training. In this categorical case, we propose for the masking of X_j to extend the levels \mathcal{A}_j by a fictitious level a_{K+1} whose embedding weight is initialized for gradient descent fitting by $\mathbf{b}_{K+1} = \mathbf{0} \in \mathbb{R}^b$.

3 Example: variable importance

3.1 Data, predictive model and conditional expectation network

We apply this conditional expectation network proposal to the French motor third party liability (MTPL) claims frequency example studied, e.g., in Charpentier [6], Lindholm et al. [20] and Wüthrich–Merz [36]; this data set is available through the R package `CASdatasets` [9]. Listing 1 gives an excerpt of the data. We use the data pre-processing as described in Chapter 13 of [36], and we choose the same network architecture as presented in Example 7.10 of [36], with entity embeddings of dimension $b = 2$ for the categorical features `VehBrand` and `Region`, see Listing 7.4 of [36]. We fit this network architecture to the available data (using early stopping) which gives us the expected frequency regression function $\mathbf{x} \mapsto \mu(\mathbf{x})$. Note that this data describes a claims frequency example, which is usually modeled with a Poisson rate regression. Therefore, we use the Poisson deviance loss, denoted by L , for model fitting and evaluation. The time exposures are used as weights in model fitting and evaluation; for the Poisson deviance loss we refer to Example 2.24 in [36].

Listing 1: Excerpt of the French MTPL claims frequency data set.

```

1 'data.frame':  678007 obs. of  12 variables:
2 $ IDpol      : num  1 3 5 10 11 13 15 17 18 21 ...
3 $ Exposure   : num  0.1 0.77 0.75 0.09 0.84 0.52 0.45 0.27 0.71 0.15 ...
4 $ Area       : Factor w/ 6 levels "A","B","C","D",...: 4 4 2 2 2 5 5 3 3 2 ...
5 $ VehPower   : int   5 5 6 7 7 6 6 7 7 7 ...
6 $ VehAge     : int   0 0 2 0 0 2 2 0 0 0 ...
7 $ DrivAge    : int  55 55 52 46 46 38 38 33 33 41 ...
8 $ BonusMalus: int   50 50 50 50 50 50 50 68 68 50 ...
9 $ VehBrand   : Factor w/ 11 levels "B1","B2","B3",...: 9 9 9 9 9 9 9 9 9 ...
10 $ VehGas     : Factor w/ 2 levels "Diesel","Regular": 2 2 1 1 1 2 2 1 1 1 ...
11 $ Density    : int  1217 1217 54 76 76 3003 3003 137 137 60 ...
12 $ Region     : Factor w/ 22 levels "R11","R21","R22",...: 18 18 3 15 15 8 8 20 20 12 ...
13 $ ClaimNb    : num   0 0 0 0 0 0 0 0 0 0 ...

```

	Poisson deviance losses	
	in-sample on \mathcal{L}	out-of-sample on \mathcal{T}
(0) null model μ_0 (empirical mean on \mathcal{L})	25.213	25.445
(1) full neural network model $\mu(\mathbf{x})$	23.777	23.849
(2) approximation $\text{NN}_{\hat{\vartheta}}(\mathbf{m})$ of null model	25.213	25.446
(3) approximation $\text{NN}_{\hat{\vartheta}}(\mathbf{x})$ full model	23.802	23.847

Table 1: Conditional expectation network approximation; Poisson deviance losses L in 10^{-2} .

The fitted model $\mu(\mathbf{x})$ and its out-of-sample performance are shown on line (1) of Table 1. These results are directly comparable to Table 7.4 in [36] because we use the same learning and test data split for the sets \mathcal{L} and \mathcal{T} , respectively; see Listing 5.2 and Table 5.2 in [36].¹ Line (0) of Table 1 shows the null model which uses the empirical mean for μ_0 . The relative increase in out-of-sample Poisson deviance loss L on \mathcal{T} when moving from the full to the null model is

$$\frac{\frac{1}{n} \sum_{i=1}^n L(Y_i, \mu_0)}{\frac{1}{n} \sum_{i=1}^n L(Y_i, \mu(\mathbf{x}_i))} - 1 = \frac{25.445}{23.849} - 1 = 6.70\%. \quad (3.1)$$

This is a comparably small value which expresses that we work in a low signal-to-noise ratio situation, which is rather typical in actuarial problems. This relative increase (3.1) is the benchmark that we are going to attribute to the different feature components.

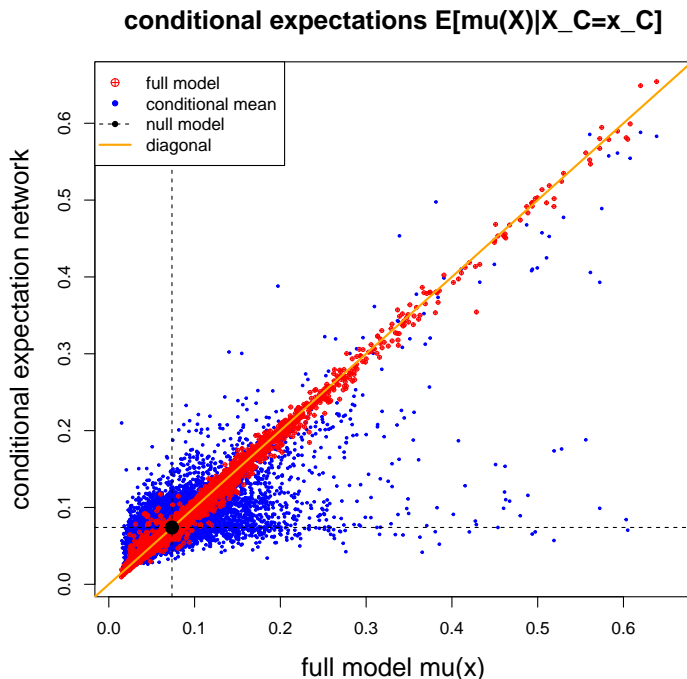


Figure 1: Conditional expectation network fitting results.

We fit the same network architecture for the calculation of the conditional expectations (2.1), and we initialize the gradient descent model fitting with the weights of the first network μ . This is precisely done as in (2.7) with the random masking as described in the previous section. Figure 1 shows the results. The red dots in Figure 1 reflect the approximation of the full model $\mu(\mathbf{x}_i)$, and a perfect network fit of $\text{NN}_{\hat{\mathcal{Q}}}(\mathbf{x}_i)$, $1 \leq i \leq n$, will set all red dots precisely on the diagonal orange line. The black dot reflects the approximation of the null model μ_0 , and $\text{NN}_{\hat{\mathcal{Q}}}(\mathbf{m})$ lies perfectly on the diagonal line. The blue dots reflect the conditional expectations $\mu_{\mathcal{C}_i}(\mathbf{x}_i)$ estimated by $\text{NN}_{\hat{\mathcal{Q}}}(\mathbf{x}_{i,\mathcal{C}_i}^{(m)})$, where the components $\mathcal{C}_i^c = \mathcal{Q} \setminus \mathcal{C}_i$ have been masked. We

¹There are small numerical differences between the results on line (1) of Table 1 and Table 7.4 in [36] because here we have standardized the continuous feature components to be centered and have unit variance, whereas as in [36] we have used the MinMaxScaler for pre-processing the continuous feature components, see (7.29)-(7.30) of [36]. Often standardization provides slightly superior results over the MinMaxScaler pre-processing.

observe that these blue dots fluctuate quite wildly, of course, this is expected as we neglect the information in the components $\mathbf{X}_{\mathcal{C}_i^c}$.

Lines (2) and (3) of Table 1 show the performance of this approximation $\text{NN}_{\hat{\mathcal{D}}}$ in the cases of the full model and of the null model. Note that the fitting procedure has only taken place on the learning data \mathcal{L} , and the disjoint sample \mathcal{T} is only used for the out-of-sample performance assessment. We observe some in-sample differences, which is a sign that the first network μ is in-sample overfitting, because the out-of-sample performance is equally good between μ and $\text{NN}_{\hat{\mathcal{D}}}$. This is interpreted that the conditional expectation network $\text{NN}_{\hat{\mathcal{D}}}$ is a regularized version of the first neural network μ , and the masked inputs act as drop-out regularization; indeed, besides for using the conditional expectation network for explanation, the good out-of-sample performance means that this network can also be used for prediction. Thus, the fitted network (2.5) seems to be a good approximation to the (conditional) means in the cases of the full and the null model.

3.2 drop1 and anova analyses

We perform a **drop1** analysis, i.e., we simply set one column of the design matrix to the mask value, similar to the one used for GLMs; differences are described at the end of this section. The full model μ , given by (2.3), dominates in convex order any model for $j \in \mathcal{Q}$

$$\mu_{\mathcal{Q} \setminus \{j\}}(\mathbf{x}) = \mathbb{E} [\mu(\mathbf{X}) | \mathbf{X}_{\mathcal{Q} \setminus \{j\}} = \mathbf{x}_{\mathcal{Q} \setminus \{j\}}] = \mathbb{E} [Y | \mathbf{X}_{\mathcal{Q} \setminus \{j\}} = \mathbf{x}_{\mathcal{Q} \setminus \{j\}}],$$

where we drop the j -th component from the information set. On the out-of-sample data \mathcal{T} , we analyze the relative increase in Poisson deviance loss L using this more crude regression function; if we drop all components we obtain (3.1) for the null model. We define on the out-of-sample data \mathcal{T} the **drop1** statistics for $j \in \mathcal{Q}$

$$\mathbf{drop1}_j = \frac{\frac{1}{n} \sum_{i=1}^n L(Y_i, \mu_{\mathcal{Q} \setminus \{j\}}(\mathbf{x}_i))}{\frac{1}{n} \sum_{i=1}^n L(Y_i, \mu(\mathbf{x}_i))} - 1. \quad (3.2)$$

Figure 2 (lhs) shows the results. Dropping the variable **BonusMalus** leads to the biggest increase in out-of-sample loss of 4.50%, compare to (3.1), and we conclude that this is the most important variable in this prediction problem (using a **drop1** analysis). At the other end, **Density** and **Area** do not seem to be important, and may be dropped from the analysis. In fact, $\mathbf{drop1}_{\text{Density}} = 0.04\% > 0$ is slightly positive and $\mathbf{drop1}_{\text{Area}} = -0.01\% < 0$ is negative (out-of-sample). The latter says that we should (clearly) drop the **Area** component from the feature \mathbf{X} , because inclusion of **Area** negatively impacts the out-of-sample performance.

We compare these **drop1** importances to the variable permutation importance (VPI) figures of Breiman [4]. VPI randomly permutes one component of the features $(\mathbf{x}_i)_{i=1}^n$ at a time across the entire sample, and then studies the change in out-of-sample loss compared to the full model. The corresponding results are shown in Figure 2 (rhs); we keep the same order on the y -axis. We observe bigger magnitudes and also a slightly different ordering compared to the **drop1** analysis. The difficulty with the VPI analysis is that it does not properly respect the dependence structure between the feature components of $\mathbf{X} \sim \pi$, e.g., if two feature components are colinear we cannot randomly permute one component across the entire portfolio without changing the other one correspondingly. In Figure 3 we show the existing dependence in our example between **DriveAge** and **BonusMalus** (lhs) and between **Area** and **Density** (rhs). For instance, we cannot change

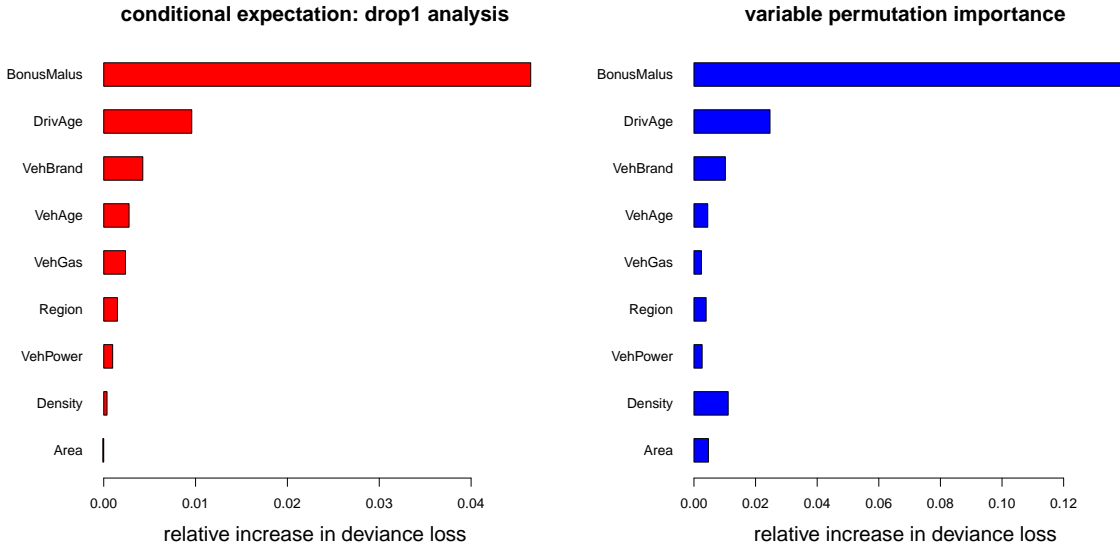


Figure 2: (lhs) Conditional expectation network for `drop1j`; importances of individual components $j \in \{\text{BonusMalus}, \dots, \text{Area}\}$, (rhs) variable permutation importance (VPI) of Breiman [4]; the x -scale differs and the order on the y -axis is the same.

the `Area` code from A to D without changing `Density` correspondingly. This is precisely done in our `drop1` analysis using the conditional expectations $\mu_{\mathcal{Q} \setminus \{j\}}(\mathbf{x})$, but it is not done in VPI. Therefore, the conditional expectation results are more reliable to measure variable importance in this case.

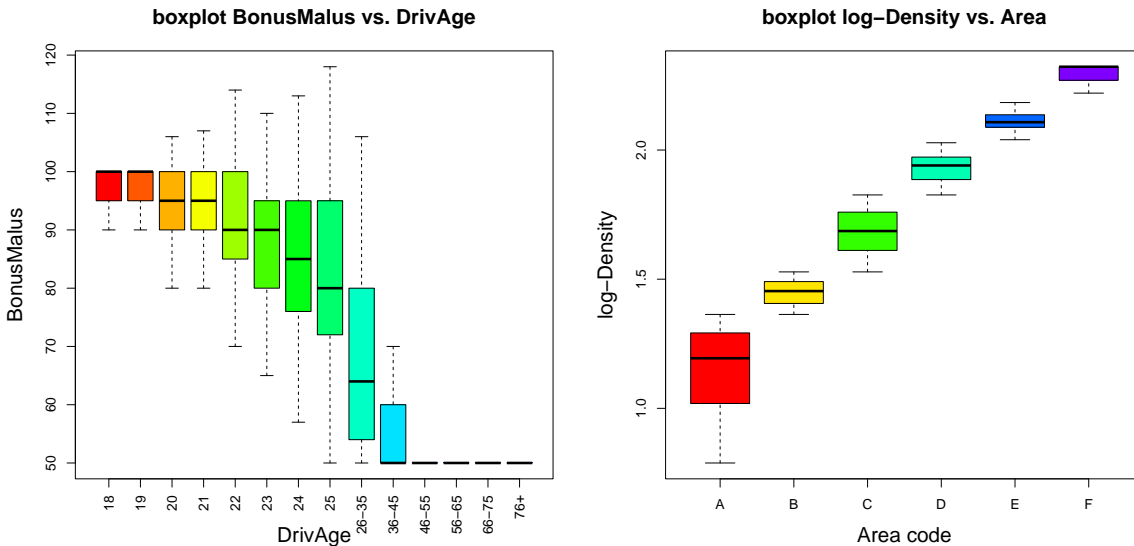


Figure 3: Dependence between the feature components of $\mathbf{X} \sim \pi$: (lhs) `DrivAge` and `BonusMalus`, and (rhs) `Area` code and `Density`; this plot is taken from Figure 13.12 in [36]; the plots only show the whiskers but not the outliers.

Moreover, since there are no young car drivers (below age 25) who are on the lowest bonus-malus level of 50%, see Figure 3 (lhs), the (fitted) regression function $\mathbf{x} \mapsto \mu(\mathbf{x})$ is not (well-)specified

for such feature values, in fact it is undefined on this part of the feature space. Therefore, we can extrapolated μ arbitrarily to this part of the feature space because this extrapolation cannot be back-tested on data. Precisely this problem questions the magnitudes in the VPI plot, because different extrapolations give us different magnitudes of increases in deviance losses.

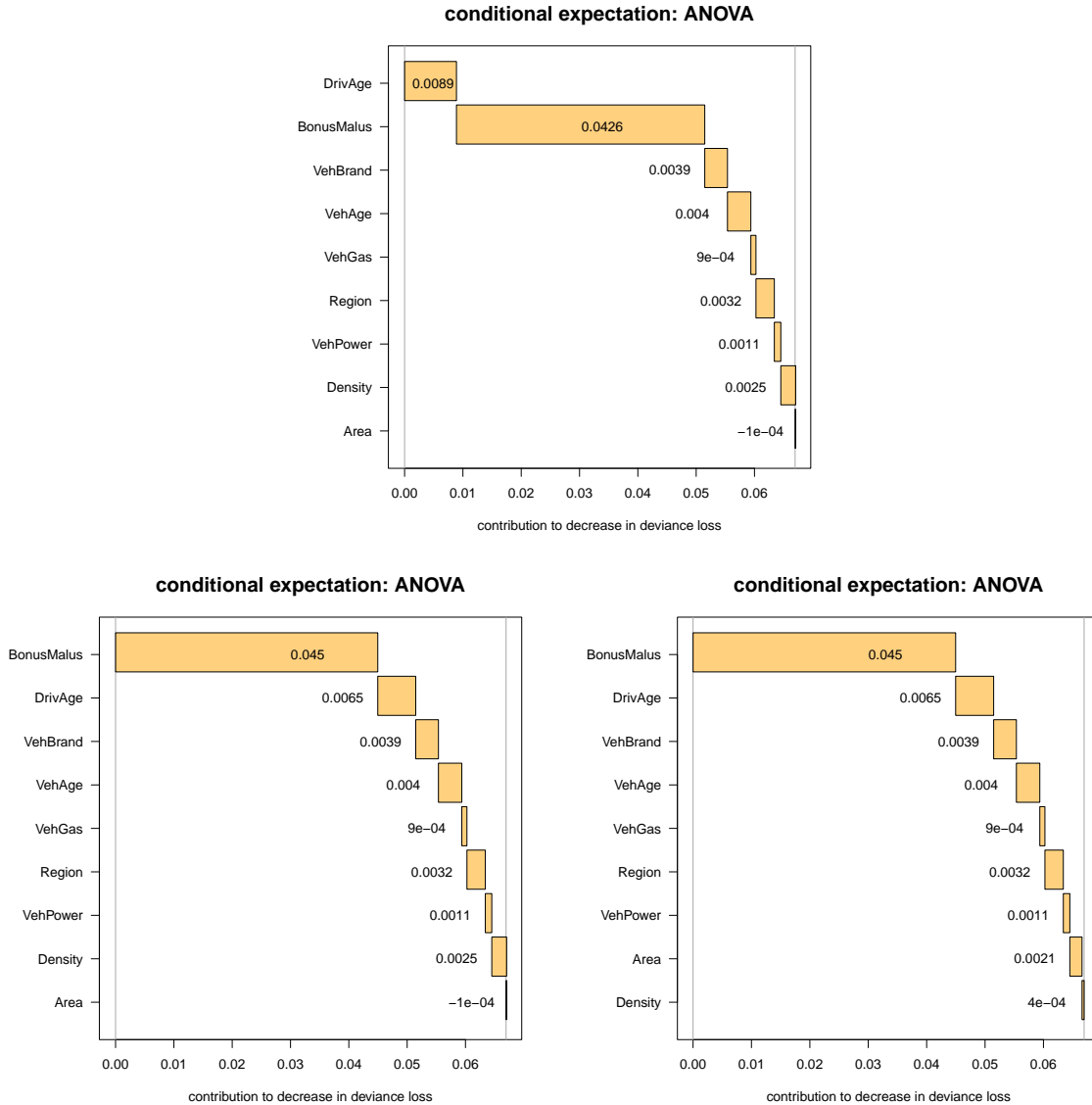


Figure 4: anova analyses for different orderings for $j \in \mathcal{Q}$ of the feature components.

Next, we study an **anova** analysis, similarly to the one offered in the R package for GLMs; we also refer to Section 2.3.2 in McCullagh–Nelder [28]. The **anova** analysis recursively adds feature components to the regression model, and analyzes the change of (out-of-sample) deviance loss provided by the inclusion of each new feature component. To have the same units as in the previous analyses we scale these changes of deviance losses with the loss of the full model, precisely as in (3.1) and (3.2). The **anova** analysis then gives us an additive decomposition of the total gap in losses between the full and null model, i.e., it explains the difference of 6.70% given in (3.1). For this we choose a sequence of mutually different indices $j_1, \dots, j_q \in \mathcal{Q}$, and

we define the contribution of feature component X_{j_k} to the decrease in deviance loss by

$$\mathbf{anova}_{j_k} = \frac{\frac{1}{n} \sum_{i=1}^n L(Y_i, \mu_{\{j_1, \dots, j_{k-1}\}}(\mathbf{x}_i)) - L(Y_i, \mu_{\{j_1, \dots, j_k\}}(\mathbf{x}_i))}{\frac{1}{n} \sum_{i=1}^n L(Y_i, \mu(\mathbf{x}_i))}, \quad (3.3)$$

for $k = 1, \dots, q$; for the first term $k = 1$ in (3.3) we set $\mu_\emptyset(\mathbf{x}) = \mu_0$. This gives us an additive decomposition of (3.1), i.e.,

$$\sum_{k=1}^q \mathbf{anova}_{j_k} = \frac{\frac{1}{n} \sum_{i=1}^n L(Y_i, \mu_0)}{\frac{1}{n} \sum_{i=1}^n L(Y_i, \mu(\mathbf{x}_i))} - 1 = \frac{25.445}{23.849} - 1 = 6.70\%.$$

Moreover, we have $\mathbf{anova}_{j_q} = \mathbf{drop1}_{j_q}$, this is the last included component $j_q \in \mathcal{Q}$. Figure 4 (top) shows the waterfall graph of the **anova** analysis stating the corresponding decreases in losses in the plot, e.g., $\mathbf{anova}_{j_1} = 0.89\%$ for $j_1 = \mathbf{DriveAge}$. We observe that by far the biggest contribution is provided by **BonusMalus**, which gives us the same conclusion about variable importance as Figure 2. The difficulty with the **anova** analysis is that the contributions depend on the order j_1, \dots, j_q of the inclusion of the feature components. In Figure 4 (bottom-lhs) we exchange the order of **DriveAge** and **BonusMalus**, and then $\mathbf{anova}_{j_2} = 0.65\% < 0.89\%$ for $j_2 = \mathbf{DriveAge}$, because part of the decrease of loss has already been explained by **BonusMalus** (through the dependence in \mathbf{X} and the interactions in the regression function μ). This is also important for dropping variables. In Figure 2, the two variables **Density** and **Area** provide the smallest values for $\mathbf{drop1}_j$. However, we also know that these two components are almost colinear, see Figure 3 (rhs). Figure 4 (bottom) verifies that one of these two components should be included in the model, (bottom-lhs) considers the order **Density-Area** and (bottom-rhs) the order **Area-Density**. Integrating the first of these two variables in position $q - 1$ into the model gives a higher contribution than the two other variables **VehPower** or **VehGas**, being considered first. Therefore, **Density/Area** is more important than these two other variables, but integration of one of them is sufficient.

Discussion and comparison to drop1 and anova analyses in GLMs.

There is an important difference between the **anova** analysis offered by GLMs and our **anova** analysis. We discuss this. The **anova** analysis for GLMs compares (two) nested GLMs. The null hypothesis states that the smaller GLM is sufficient against the alternative hypothesis that we should work in a bigger GLM including more components. Having nested GLMs, this hypothesis can be tested using a likelihood ratio test (LRT). The starting point of this test is the hypothesis that the smaller GLM is sufficient.

Our **anova** analysis starts from the bigger model that specifies a regression function $\mathbf{x} \mapsto \mu(\mathbf{x})$, and the smaller models are obtained by considering conditional expectations of that regression function. This provides (a sort of) nested models, but typically these nested models will not be of the same type. E.g., if we start with a GLM with log-link function we have regression function

$$\mathbf{x} \mapsto \mu(\mathbf{x}) = \exp \left\{ \beta_0 + \sum_{j=1}^q \beta_j x_j \right\},$$

for regression parameter $\boldsymbol{\beta} = (\beta_0, \dots, \beta_q)^\top \in \mathbb{R}^{q+1}$. If we drop the last component we receive

$$\begin{aligned} \mu_{\mathcal{Q} \setminus \{q\}}(\mathbf{x}) &= \mathbb{E} [\mu(\mathbf{X}) | \mathbf{X}_{\mathcal{Q} \setminus \{q\}} = \mathbf{x}_{\mathcal{Q} \setminus \{q\}}] \\ &= \exp \left\{ \beta_0 + \sum_{j=1}^{q-1} \beta_j x_j \right\} \mathbb{E} [\exp\{\beta_q X_q\} | \mathbf{X}_{\mathcal{Q} \setminus \{q\}} = \mathbf{x}_{\mathcal{Q} \setminus \{q\}}]. \end{aligned}$$

This last conditional expectation can have any functional form in $\mathbf{x}_{\mathcal{Q} \setminus \{q\}}$, and we do not necessarily have a GLM for this reduced model.

3.3 Marginal conditional expectation plot

A very popular visual explainability tool in machine learning is the PDP. The PDP has been introduced and studied by Friedman [10] and Zhao–Hastie [37]. PDPs marginalize the regression function $\mu(\mathbf{X})$ for all components X_j of \mathbf{X} , $j \in \mathcal{Q}$, by considering an unconditional expectation

$$x_j \mapsto \mathbb{E} [\mu(\mathbf{X}_{\mathcal{Q} \setminus \{j\}}, x_j)]. \quad (3.4)$$

The unconditional expectation (3.4) sets the j -th component of the feature equal to x_j , and averages over the remaining feature components $\mathbf{X}_{\mathcal{Q} \setminus \{j\}}$ without considering the correct dependence structure between $\mathbf{X}_{\mathcal{Q} \setminus \{j\}}$ and $X_j = x_j$. That is, equivalently to VPI in Figure 2 (rhs), the true dependence structure is neglected in (3.4), and it precisely suffers the same deficiency because we may average over feature combinations that do not occur in the data, e.g., due to colinearity. This issue is generally criticized in the literature; see, e.g., Apley–Zhu [2]. Based on the estimated conditional expectation network $\text{NN}_{\hat{\theta}}$, we can easily correct for this deficiency by considering the marginal conditional expectations, for $j \in \mathcal{Q}$,

$$x_j \mapsto \mu_{\{j\}}(\mathbf{x}) = \mathbb{E} [\mu(\mathbf{X}) | X_j = x_j] = \mathbb{E} [Y | X_j = x_j]. \quad (3.5)$$

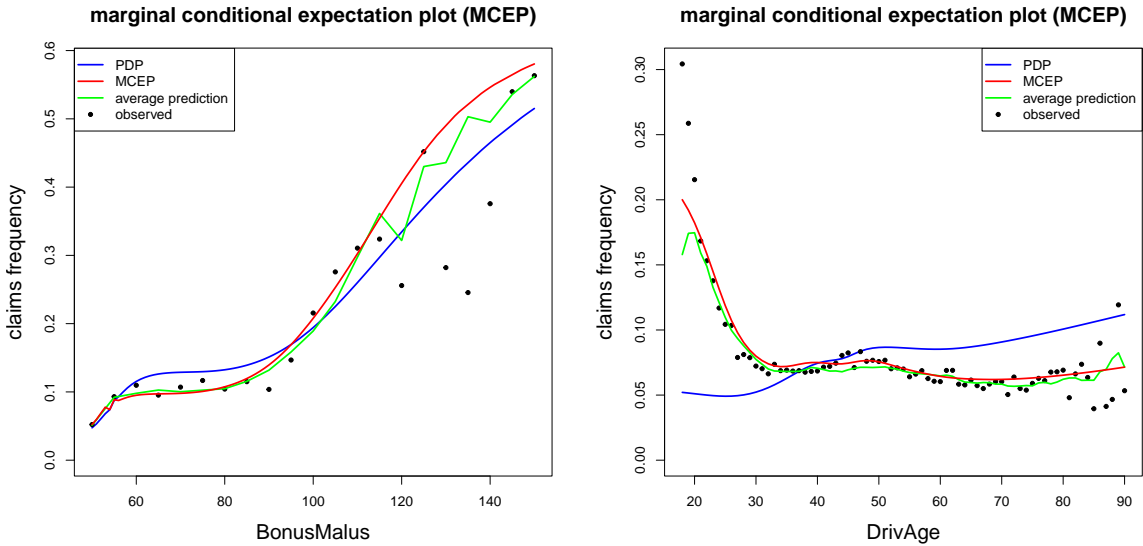


Figure 5: PDP (3.4) and MCEP (3.5): (lhs) variable `BonusMalus`, and (rhs) variable `DrivAge`.

Figure 5 shows the PDPs (3.4) and the MCEPs (3.5) for the two different feature components $j = \text{BonusMalus}$ on the (lhs) and $j = \text{DrivAge}$ on the (rhs). The blue lines give the PDPs and

the red lines the MCEPs. These lines are complemented by the empirical observations (black dots) and the average prediction (green lines) given by, respectively,

$$\bar{y}_{c_j} = \frac{\sum_{i=1}^n Y_i \mathbb{1}_{\{x_{i,j}=c_j\}}}{\sum_{i=1}^n \mathbb{1}_{\{x_{i,j}=c_j\}}} \quad \text{and} \quad \bar{\mu}_{c_j} = \frac{\sum_{i=1}^n \mu(\mathbf{x}_i) \mathbb{1}_{\{x_{i,j}=c_j\}}}{\sum_{i=1}^n \mathbb{1}_{\{x_{i,j}=c_j\}}},$$

where c_j runs over all levels that feature component X_j of \mathbf{X} can take. For the most important feature variable, $j = \text{BonusMalus}$, the red and blue lines of the MCEP and PDP look fairly similar. However, for $j = \text{DriveAge}$, the graphs look quite different for young driver ages. As described in the previous section, young car drivers cannot be on the lowest bonus-malus level of 50%, therefore, the PDP may not give reasonable results for young ages. Contrary, the MCEP can deal with such dependencies and it is verified by Figure 5 (rhs) that the red MCEP curve meets the empirical observations \bar{y}_{c_j} (black dots) quite well, which says that the marginalized conditional version (3.5) reflects a one-dimensional regression. The empirical version \bar{y}_{c_j} (black dots) is a noisy version of the average prediction $\bar{\mu}_{c_j}$ (green line), and also the average prediction and the MCEP curve are rather similar. The MCEP curve is a conditional expectation (3.5), whereas the average prediction $\bar{\mu}_{c_j}$ is a randomized version thereof, considering the empirical (realized) portfolio distribution of $(\mathbf{x}_i)_{i=1}^n$.

4 Example: SHAP

4.1 Additive and fair decomposition

We discuss SHAP in this section. SHAP is a popular model-agnostic explainability tool for (complex) regression models, see Lundberg–Lee [24] and Aas et al. [1], but it is also increasingly used to solve other decomposition and attribution problems, e.g., a risk allocation example in pension insurance is given by Godin et al. [12]. SHAP is motivated by cooperative game theory. Shapley [32] stated the following axioms for sharing common gains and costs in an additive and fair way within a cooperation of $q \geq 2$ players. The **anova** analysis (3.3) has provided an additive decomposition of the total loss gap between the full and the null model, but the **anova** decomposition cannot be considered to be fair, because the order of the inclusion matters in **anova**, see Figure 4.

Assume there exists a value function ν that maps from the power σ -algebra of \mathcal{Q} to the real line, i.e.,

$$\nu : \mathcal{C} \subseteq \mathcal{Q} \mapsto \nu(\mathcal{C}) \in \mathbb{R}. \quad (4.1)$$

This value function $\nu(\mathcal{C})$ measures the contribution of each coalition $\mathcal{C} \subseteq \mathcal{Q}$ to the total payoff given by $\nu(\mathcal{Q})$. Shapley [32] postulated the following four axioms to be desirable properties of an additive and fair distribution $(\mu_j)_{j=1}^q = (\mu_j^{(\nu)})_{j=1}^q$ of the total payoff $\nu(\mathcal{Q})$ among the q players; see also Aas et al. [1]:

- (A1) *Efficiency*: $\nu(\mathcal{Q}) - \nu(\emptyset) = \sum_{j=1}^q \mu_j$. Set $\mu_0 = \nu(\emptyset)$.
- (A2) *Symmetry*: If $\nu(\mathcal{C} \cup \{j\}) = \nu(\mathcal{C} \cup \{k\})$ for every $\mathcal{C} \subseteq \mathcal{Q} \setminus \{j, k\}$, then $\mu_j = \mu_k$.
- (A3) *Dummy player*: If $\nu(\mathcal{C} \cup \{j\}) = \nu(\mathcal{C})$ for every $\mathcal{C} \subseteq \mathcal{Q} \setminus \{j\}$, then $\mu_j = 0$.
- (A4) *Linearity*: Consider two cooperative games with value functions ν_1 and ν_2 . Then, $\mu_j^{(\nu_1 + \nu_2)} = \mu_j^{(\nu_1)} + \mu_j^{(\nu_2)}$ and $\mu_j^{(\alpha \nu_1)} = \alpha \mu_j^{(\nu_1)}$ for all $1 \leq j \leq q$ and $\alpha \in \mathbb{R}$.

The so-called *Shapley values* [32] are the only solution to distribute a total payoff $\nu(\mathcal{Q})$ among the q players so that these four axioms (A1)–(A4) are fulfilled, and they are given for each $j \in \mathcal{Q}$ by

$$\mu_j = \sum_{\mathcal{C} \subseteq \mathcal{Q} \setminus \{j\}} \frac{|\mathcal{C}|! (q - |\mathcal{C}| - 1)!}{q!} \left[\nu(\mathcal{C} \cup \{j\}) - \nu(\mathcal{C}) \right]; \quad (4.2)$$

we refer to formula (4) in Lundberg–Lee [24].

There remain two important questions:

- (1) How should the value function (4.1) be chosen if we translate the cooperative game theoretic result to regression modeling, meaning that we would like to “share” a prediction $\mu(\mathbf{x})$ in a fair and additive way (axioms (A1)–(A4)) among the feature components of \mathbf{x} ?
- (2) How can (4.2) be calculated efficiently?

Item (2) has been answered in Theorem 2 of Lundberg–Lee [24], namely, the Shapley value can be obtained by solving the following constraint weighted square loss minimization problem

$$\arg \min_{(\mu_j)_{j=1}^q} \sum_{\emptyset \neq \mathcal{C} \subseteq \mathcal{Q}} \frac{q - 1}{\binom{q}{|\mathcal{C}|} |\mathcal{C}| (q - |\mathcal{C}|)} \left(\nu_0(\mathcal{C}) - \sum_{j \in \mathcal{C}} \mu_j \right)^2, \quad \text{subject to } \sum_{j=1}^q \mu_j = \nu_0(\mathcal{Q}), \quad (4.3)$$

where we define $\nu_0(\mathcal{C}) = \nu(\mathcal{C}) - \nu(\emptyset)$, and where we set $\mu_0 = \nu(\emptyset)$. This approach is commonly known as KernelSHAP in the literature, and the term before the square bracket in (4.3) is called Shapley kernel weight. Optimization (4.3) states a convex minimization problem with a linear side constraint which can be solved with the method of Lagrange. For computing (4.3) simultaneously for different instances (different value functions ν , see also (4.5), below), a more efficient way is to include the side constraint in a different (approximate) way by extending the summation in (4.3) by the term $\mathcal{C} = \mathcal{Q}$. This extension gives a Shapley kernel weight of $+\infty$, and to deal with this undefined value, one simply sets the Shapley kernel weight for the term $\mathcal{C} = \mathcal{Q}$ to a very large value; see, e.g., Section 2.3.1 of Aas et al. [1]. The optimal solution in that case is given by

$$(\mu_j)_{j=1}^q = \left(Z^\top W Z \right)^{-1} Z^\top W \boldsymbol{\nu}, \quad (4.4)$$

with diagonal Shapley kernel weight matrix $W \in \mathbb{R}^{(2^q - 1) \times (2^q - 1)}$, vector $\boldsymbol{\nu} \in \mathbb{R}^{2^q - 1}$ containing all terms $\nu_0(\mathcal{C}) = \nu(\mathcal{C}) - \nu(\emptyset)$ of all coalitions $\emptyset \neq \mathcal{C} \subseteq \mathcal{Q}$, and design matrix $Z \in \{0, 1\}^{(2^q - 1) \times q}$. Note that if one considers different instances (different value functions ν), only the last term $\boldsymbol{\nu}$ in (4.4) changes, and the remaining terms only need to be calculated once.

The summation in (4.3) involves $2^q - 2$ terms which can be large for high-dimensional features \mathbf{X} . Therefore, in applications, one often uses a randomized version of (4.3) that randomly samples the terms of the summation in (4.3) with categorical probabilities determined by the Shapley kernel weights; we refer to Section 2.3.1 in Aas et al. [1]. This solves item (2) from above.

Item (1) is more controversial. The Shapley values (4.2) are unique for a given value function choice (4.1). Lundberg–Lee [24] have proposed to choose as value function the conditional expectations for a given instance $\mathbf{x} \in \mathcal{X}$. That is, for a selected \mathbf{x} , we define the value function

$$\mathcal{C} \subseteq \mathcal{Q} \mapsto \nu(\mathcal{C}) := \mu_{\mathcal{C}}(\mathbf{x}) = \mathbb{E}[\mu(\mathbf{X}) | \mathbf{X}_{\mathcal{C}} = \mathbf{x}_{\mathcal{C}}], \quad (4.5)$$

see (2.1). In the case of tree based regressions, a version of these Shapley values can efficiently be calculated using the so-called TreeSHAP method of Lundberg et al. [23]. However, in the general case, there has not been any efficient way of calculating the conditional expectations (4.5) and the Shapley values, respectively. Therefore, the conditional expectations (4.5) have been replaced by approximations, see formula (11) in Lundberg–Lee [24],

$$\nu(\mathcal{C}) := \mathbb{E} [\mu(\mathbf{X}_{\mathcal{Q}\setminus\mathcal{C}}, \mathbf{x}_{\mathcal{C}})], \quad (4.6)$$

i.e., similarly to VPI in Figure 2 (rhs) and the PDP (3.4), the true dependence structure between $\mathbf{X}_{\mathcal{Q}\setminus\mathcal{C}}$ and $\mathbf{X}_{\mathcal{C}}$ is neglected in (4.6); sometimes this is also called interventional SHAP, see Laberge–Pequignot [19]. In fact, (4.5) and (4.6) are equal if $\mathbf{X}_{\mathcal{Q}\setminus\mathcal{C}}$ and $\mathbf{X}_{\mathcal{C}}$ are independent. In our example, this is clearly not the case, see Figure 3. This is also the main issue raised in Aas et al. [1], and as an improvement, these authors propose Gaussian approximations to the true dependence structure. In our example, we directly approximate the conditional expectations using the estimated network $\text{NN}_{\hat{\mathcal{G}}}$, see (2.7), i.e., we perform a conditional SHAP using the surrogate network $\text{NN}_{\hat{\mathcal{G}}}$ for fast computation.

The concept of using the conditional expectations (2.1) has been criticized as a whole in the paper of Sundararajan–Najmi [33] showing that in some situations this choice leads to unreasonable Shapley values $(\mu_j)_{j=0}^q$, and these authors propose to use an unconditional expectation (4.6) in general. This proposal is also supported by causal arguments given in Janzing et al. [16]. However, causal arguments often use strong assumptions that cannot easily be verified, e.g., the exclusion of unmeasured confounders, and the general use of an unconditional expectation (4.6) cannot be supported in situations like the ones in Figure 3. Namely, in this example, there are no car drivers with `DrivAge` below 25 having a `BonusMalus` level of 50%. Therefore, the regression function $\mu(\mathbf{x})$ is undetermined for such features \mathbf{x} and, henceforth, (4.6) cannot generally be calculated because the specific value of one variable leads to constraints in the support of the other variable. This problem can be circumvented by extending the regression function μ to this part of the feature space, however, this extension is completely subjective because it cannot be supported and verified by data. In the examples in the next section, we compare the conditional and unconditional versions (4.5) and (4.6), respectively, and for the extrapolation, we simply use the one provided by the fitted neural network.

We remark that there is interesting work that extends Shapley values to higher order decompositions and representations; we refer to Tsai et al. [34] and Hiabu et al. [15]. The basic idea is to give a functional decomposition of the regression function by including higher interaction terms. This can partly mitigate the difficulty of the decision whether one should work with conditional or unconditional expectations, however, some issues remain, e.g., the above mentioned support constraints cannot be dealt with the (unconstrained) marginal identification given by formula (2) in Hiabu et al. [15].

4.2 SHAP for mean decompositions

We apply the SHAP explanation to the regression value $\mu(\mathbf{x})$ of a given instance \mathbf{x} . We compare the conditional and unconditional versions (4.5) and (4.6), respectively. For the unconditional version and its graphical illustrations we use the R packages `kernelshap` [27] and `shapviz` [26]; we refer to Mayer et al. [25] for more description.

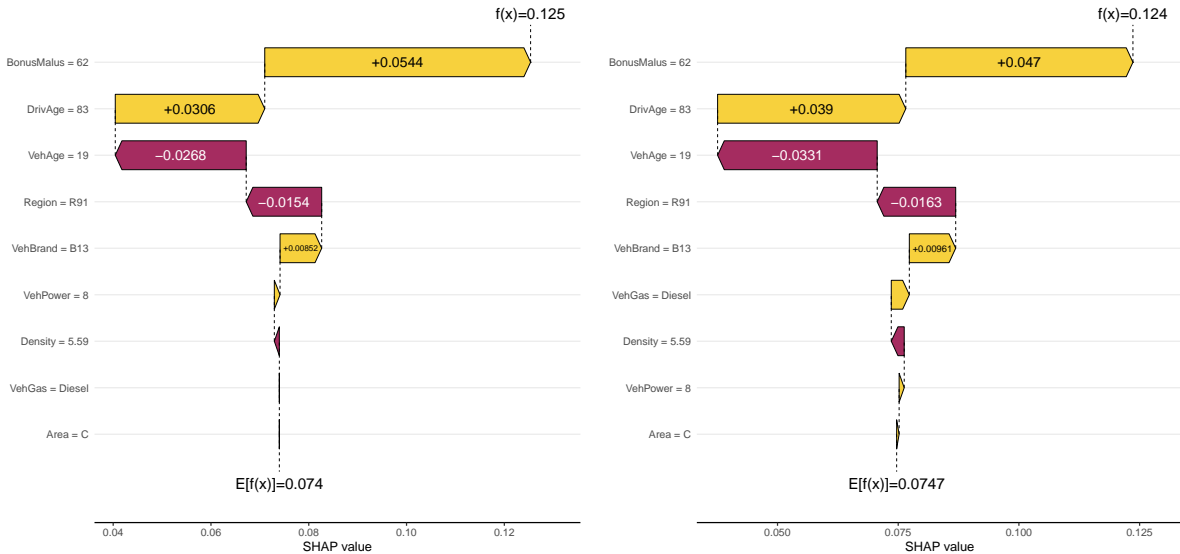


Figure 6: Waterfall graphs of the Shapley decomposition $(\mu_j)_{j=0}^q$ of $\mu(\mathbf{x})$ of a selected instance $\mathbf{x} \in \mathcal{X}$: (lhs) conditional expectation (4.5) for value function ν ; (rhs) unconditional expectation (4.6) for value function ν ; these waterfall graphs use `shapviz` [26].

Figure 6 shows the waterfall graphs of the Shapley decomposition $(\mu_j)_{j=0}^q$ of $\mu(\mathbf{x})$ of a given instance with features $\mathbf{x} \in \mathcal{X}$; the ordering on the y -axis is according to the sizes of these Shapley values $(\mu_j)_{j=1}^q$. The left-hand side shows the conditional version (4.5) and the right-hand side the unconditional one (4.6). These conditional SHAP values with (4.5) are obtained by using the conditional expectation network $\text{NN}_{\hat{\mathcal{D}}}$ for fast computation. That is, we only need to fit one single neural network that serves at simultaneously calculating the conditional expectations of all possible subsets $\mathcal{C} \subseteq \mathcal{Q}$. A naive way would be to fit a network to each subset, which would require to fit 2^q networks.

The results in Figure 6 are rather similar in this example, and there does not seem to be an issue with the colinearities illustrated in Figure 3, because **Density/Area** only has a marginal influence on regression value $\mu(\mathbf{x})$ and **DrivAge/BonusMalus** is not in the critical (undetermined) part of the feature space.

In Figure 7 we give a second example of a young car driver of age **DrivAge** = 20. Car drivers enter a bonus-malus scheme at level 100%, and every year of accident-free driving decreases this level by 5% (and an accident increases the bonus-malus level by a fixed percentage). Thus, it takes at least 10 years of accident-free driving until a car driver can reach the lowest bonus-malus level of 50%.² As a result, the regression function μ is undetermined for features having **DrivAge** = 20 and **BonusMalus** < 90%, and we can assign any value to μ for this feature as it does not occur in the data. This is precisely what is happening when using the unconditional version (4.6) for SHAP, and in Figure 7 (rhs) we observe that **BonusMalus** gets a large attribution if we just extrapolate the (first) neural network regression function μ to that part of the feature space. Of course, this cannot be justified and supported by data, as it extrapolates μ arbitrarily

²The fact that Figure 3 does not precisely reflect a 5% decrease for every accident-free year is an issue in data quality, e.g., drivers at the age of 18 can technically not be on a bonus-malus level of 90%, but there are still a few such observations in our data, which we attribute to data error.

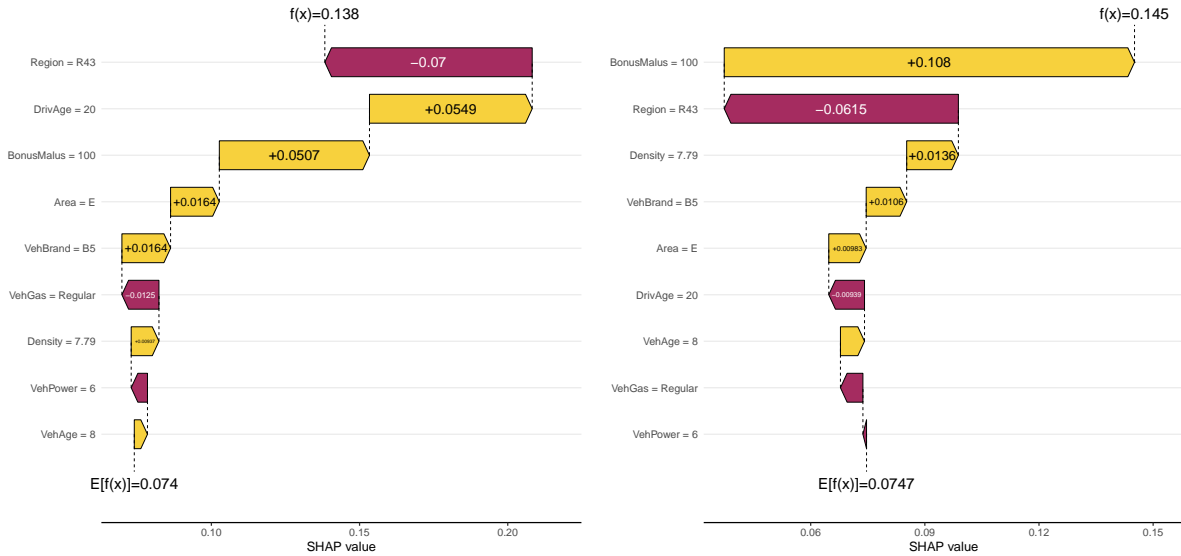


Figure 7: Waterfall graphs of the Shapley decomposition $(\mu_j)_{j=0}^q$ of $\mu(\mathbf{x})$ of a selected instance $\mathbf{x} \in \mathcal{X}$: (lhs) conditional expectation (4.5) for value function ν ; (rhs) unconditional expectation (4.6) for value function ν ; these waterfall graphs use `shapviz` [26].

to the undefined part of the feature space \mathcal{X} . In such examples, we give clear preference to the conditional version (4.5) on the left-hand side of Figure 7.

4.3 LightGBM surrogate model

We compare the SHAP mean decomposition results of the previous Section 4.2 to the corresponding TreeSHAP results by approximating the full model $\mu(\mathbf{x})$ by a LightGBM surrogate tree regression model.³ Using this LightGBM surrogate model, we study the resulting TreeSHAP mean decomposition of Lundberg et al. [23] implemented in the R package `shapviz` [26].

Figure 8 gives a scatter plot of the two feature components `DrivAge` (top) and `BonusMalus` (bottom) on the x -axis vs. their SHAP attributions on the y -axis for 1000 randomly selected cases \mathbf{x}_i ; remark that the two selected components are dependent, see Figure 3 (lhs), and they are expected to interact in the regression model. In Figure 8 we show the following SHAP mean attributions of 1000 randomly selected cases \mathbf{x}_i : (lhs) conditional mean (4.5) as value function, (rhs) unconditional mean (4.6) as value function, and (rhs) TreeSHAP LightGBM surrogate model decomposition. For the latter we use the R package `shapviz` [26], which performs the decomposition on the log-scale, therefore, we also choose the log-scale for the former two methods. The coloring in Figure 8 selects the feature component that shows the highest interaction with the selected one, i.e., explains best the vertical scattering: (top) for feature `DrivAge` this is the variable `BonusMalus`; (bottom) for feature `BonusMalus` there are different choices between the different SHAP methods. The conditional mean version (4.5) selects `DrivAge`, whereas the unconditional mean (4.6) and TreeSHAP versions select `VehBrand`; note that this categorical variable is treated differently in the network approach (embedding layers) and in the LightGBM

³To fit the LightGBM surrogate regression model, we use the same parametrization as in the model on <https://github.com/JSchellendorfer/ActuarialDataScience/tree/master/14-SHAP>; we also refer to Mayer et al. [25].

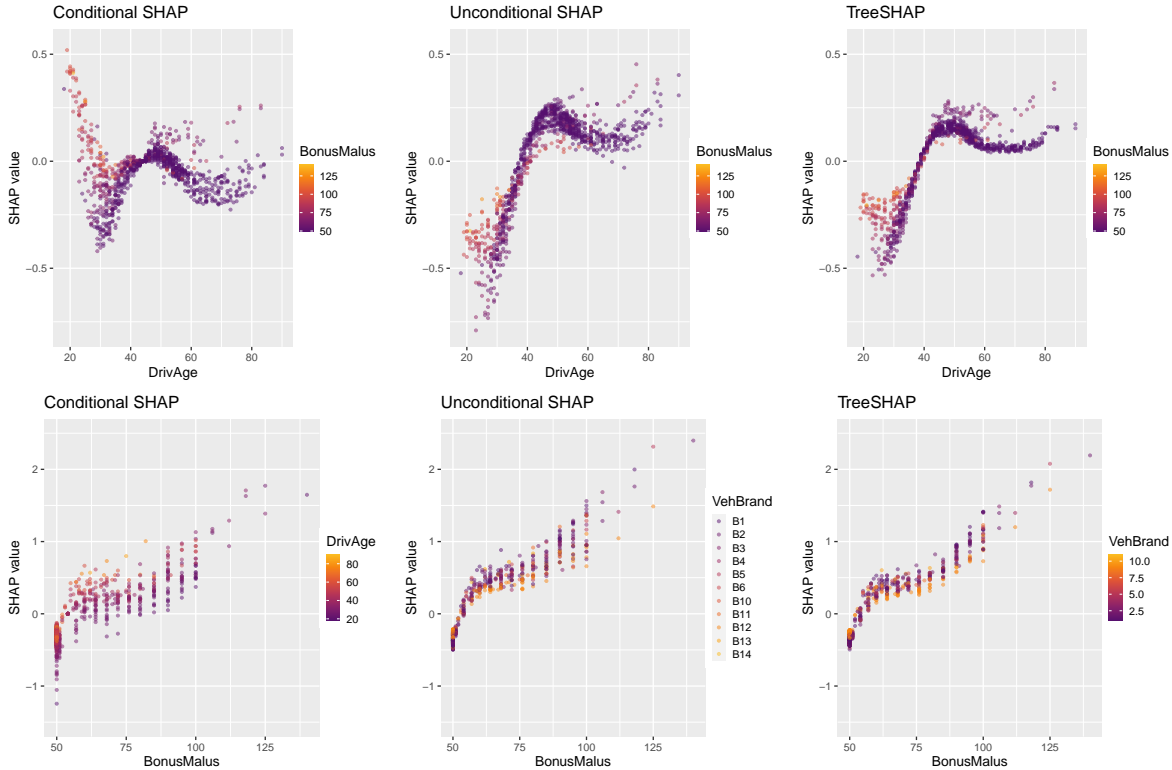


Figure 8: Dependence plots of SHAP mean decompositions: (top) `DrivAge`, (bottom) `BonusMalus`, (lhs) conditional expectation version (4.5), (middle) unconditional expectation version (4.6), (rhs) LightGBM surrogate model.

(exclusive feature bundling to bundle sparse (one-hot encoded) features). From these graphs, it seems that the unconditional mean version (4.6) and the TreeSHAP version using a surrogate LightGBM provide rather similar results, and they are different from the conditional mean version (4.5); the plots use the same scale on the y -axis. Since the unconditional version cannot cope with colinearity in feature components, we give preference to the results in the left column of Figure 8 using the conditional mean version (4.5). In particular, this is justified by the discussion in Section 4.2, namely, for small values of `DrivAge` we cannot have a low `BonusMalus` level, and any extrapolation to this part of the feature space is arbitrary (but it will impact the results of the unconditional version).

4.4 SHAP for out-of-sample deviance loss attribution

We have seen in Section 3 that the `anova` analysis depends on the order of the inclusion of the feature components, i.e., we receive an additive loss decomposition which cannot be considered to be fair, because if we change the order of inclusion of the components their importance in the `anova` analysis may change. Instead of the `anova` decomposition, we consider a Shapley deviance loss attribution in this section. For this, we choose the value function of instance \mathbf{x}_i as

$$\mathcal{C} \mapsto \nu_{(Y_i, \mathbf{x}_i)}(\mathcal{C}) := L(Y_i, \mu_{\mathcal{C}}(\mathbf{x}_i)) = L\left(Y_i, \mathbb{E}[\mu(\mathbf{X}) | \mathbf{X}_{\mathcal{C}} = \mathbf{x}_{i,\mathcal{C}}]\right), \quad (4.7)$$

where L is the Poisson deviance loss used, e.g., in (3.1), and we add the specific choice of the observation (Y_i, \mathbf{x}_i) as a lower index to the notation of the value function $\nu_{(Y_i, \mathbf{x}_i)}$. Note that we

do not decompose the regression function $\mu(\mathbf{x})$ in this section, but rather the resulting deviance loss $L(Y, \mu(\mathbf{x}))$.

For $\mathcal{C} = \emptyset$ we receive the average loss of the null model

$$\frac{1}{n} \sum_{i=1}^n L(Y_i, \mu_0) = \frac{1}{n} \sum_{i=1}^n \nu_{(Y_i, \mathbf{x}_i)}(\emptyset),$$

and for $\mathcal{C} = \mathcal{Q}$ we obtain the average loss of the full model

$$\frac{1}{n} \sum_{i=1}^n L(Y_i, \mu(\mathbf{x}_i)) = \frac{1}{n} \sum_{i=1}^n \nu_{(Y_i, \mathbf{x}_i)}(\mathcal{Q}),$$

this refers to lines (2) and (3) of Table 1. Remark that these quantities are empirical counterparts of the losses of the true random tuple (Y, \mathbf{X}) , given by for the null and the full model, respectively,

$$\mathbb{E}[L(Y, \mu_0)] = \mathbb{E}[\nu_{(Y, \mathbf{X})}(\emptyset)] \quad \text{and} \quad \mathbb{E}[L(Y, \mu(\mathbf{X}))] = \mathbb{E}[\nu_{(Y, \mathbf{X})}(\mathcal{Q})].$$

Using the Shapley decomposition of Section 4.1, we can attribute the difference in these losses to the feature components X_j of \mathbf{X} . In a first step, we therefore decompose the Poisson deviance loss $L(Y_i, \mu(\mathbf{x}_i))$ for each observation (Y_i, \mathbf{x}_i) of the test sample \mathcal{T} using the value function (4.7). This provides us for all observations (Y_i, \mathbf{x}_i) with an additive and fair decomposition giving the Shapley values $(\phi_{j, (Y_i, \mathbf{x}_i)})_{j=1}^q$ such that

$$L(Y_i, \mu(\mathbf{x}_i)) = \nu_{(Y_i, \mathbf{x}_i)}(\mathcal{Q}) = L(Y_i, \mu_0) + \sum_{j=1}^q \phi_{j, (Y_i, \mathbf{x}_i)}.$$

In a second step, we average over these decompositions to receive the average contribution (averaged over \mathcal{T}) of feature component X_j , $j \in \mathcal{Q}$, given by

$$\Phi_j = \frac{1}{n} \sum_{i=1}^n \phi_{j, (Y_i, \mathbf{x}_i)}. \quad (4.8)$$

Since the Shapley decomposition is still computationally demanding, we consider (4.8) for a random sub-sample of \mathcal{T} , otherwise one may use parallel computing.⁴

The following gives a pseudo-code for the SHAP deviance loss attribution.

-
- (0) Select at random a fixed number $m \leq 2^q - 2$ of non-empty subsets $\mathcal{C} \subset \mathcal{Q}$, and calculate for this random selection the matrix, see (4.4),

$$A = \left(Z^\top W Z \right)^{-1} Z^\top W \in \mathbb{R}^{q \times (m+1)},$$

where we additionally add the case $\mathcal{C} = \mathcal{Q}$ with a large Shapley kernel weight.

⁴To compute the Shapley decomposition of the Poisson deviance loss for 1000 observations (Y_i, \mathbf{x}_i) on an ordinary laptop (based on a neural network $\text{NN}_{\hat{\phi}}$) takes roughly 1 minute.

- (1) Select at random a fixed number n of cases i , and calculate for each case i and each selected subset \mathcal{C} from item (0) the individual deviance loss differences, see (4.7) and (2.6),

$$\widehat{\nu}_{(Y_i, \mathbf{x}_i)}^0(\mathcal{C}) = L\left(Y_i, \text{NN}_{\widehat{\theta}}(\mathbf{x}_{i, \mathcal{C}}^{(m)})\right) - L(Y_i, \mu_0). \quad (4.9)$$

This provides us with vectors $\widehat{\nu}_i = (\widehat{\nu}_{(Y_i, \mathbf{x}_i)}^0(\mathcal{C}))_{\mathcal{C} \in \mathbb{R}^{m+1}}$, considering all the subsets $\mathcal{C} \subseteq \mathcal{Q}$ selected in item (0).

- (2) Compute the approximate individual Shapley deviance loss decompositions of all selected cases i

$$(\widehat{\phi}_{j, (Y_i, \mathbf{x}_i)})_{j=1}^q = A \widehat{\nu}_i \in \mathbb{R}^q.$$

- (3) Return the estimated average attributions $\widehat{\Phi}_j = \frac{1}{n} \sum_{i=1}^n \widehat{\phi}_{j, (Y_i, \mathbf{x}_i)}$.

We give a few remarks. Matrix A in item (0) only considers the rows and columns of the Shapley kernel weight matrix W and the design matrix Z that have been chosen by the random selections $\mathcal{C} \subseteq \mathcal{Q}$, we also refer to (4.4). This is an approximation that reduces the computational complexity for large q . Item (1) uses the network approximation for the calculation of the conditional expectations (2.1). This step precisely reflects the efficiency gain of our approach because it requires only *one single* fitted neural network $\text{NN}_{\widehat{\theta}}$ to calculate the conditional expectations for all considered cases i and all selected subsets \mathcal{C} , see (4.9). Item (2) are simple matrix multiplications that always rely on the same matrix A .

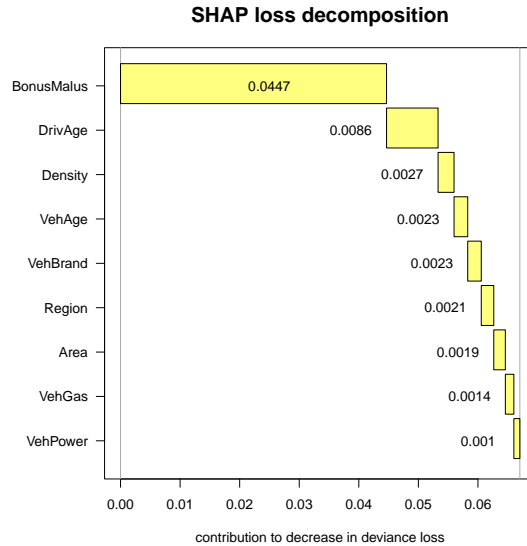


Figure 9: SHAP Poisson deviance loss decomposition $(\text{SHAP_anova}_j)_{j \in \mathcal{Q}}$.

Figure 9 shows the resulting (relative) SHAP Poisson deviance loss decomposition for, $j \in \mathcal{Q}$,

$$\text{SHAP_anova}_j = - \frac{\widehat{\Phi}_j}{\frac{1}{n} \sum_{i=1}^n L(Y_i, \mu(\mathbf{x}_i))},$$

compare to (3.3); the y -scale is in the order of the magnitudes of the decreases. This figure should be compared to the `anova` analyses of Figure 4. In contrast to these latter graphs, Figure 9 provides a variable importance ranking that is fair (in the Shapley sense and for the chosen value functions (4.7)), and it does not depend on the order of the inclusion of the feature components. E.g., we observe that the magnitudes of the contributions of `BonusMalus` and `DrivAge` are somewhere in between the values in Figure 4, where these two variables are included in different orders in this latter figure. From Figure 9 we mainly question the importance of `VehPower`, and we could rerun the models without this variable.

Another interesting observation is the importance of `Density` and `Area` which are highly colinear, see Figure 3 (rhs). Both variables receive a similar magnitude of importance, the more granular `Density` variable being slightly more important. We interpret these SHAP results in case of colinear variables as follows. These two variables share a (common) importance because they may equally contribute to the decrease in loss, i.e., we have (almost) equally behaved players in this cooperative game. Of course, this also means that the importance of a variable is diminished if we add a second colinear one to the model, and, in fact, we should work with the smaller model in that case. This is not in contradiction to the examples in Sundararajan–Najmi [33], it just says that colinearity needs to be assessed carefully before regression modeling, because the regression model may not detect this (and we should try to work in a parsimonious model already in the first place). A way of exploring colinearity is the `anova` graph of Figure 4 because changing the order of inclusion will also change the magnitudes of contribution, as can be seen from that figure for the variables `Density` and `Area`.

5 Conclusion

Starting from a regression function $\mu(\mathbf{X})$ that is based on tabular input data \mathbf{X} , we have proposed a neural network surrogate model that can calculate the conditional expectations of $\mu(\mathbf{X})$ by conditioning on any subset of components of the tabular input data \mathbf{X} . These conditional expectations are useful in different contexts. We present an `anova` and a `drop1` variable importance analysis, respectively. These analyses are similar to their generalized linear model (GLM) counterparts, except that we do not require to have nested models, here, but we start from a bigger model and calculate the smaller model. Our second example modifies the partial dependence plot (PDP) by correcting for the deficiency that PDPs cannot cope with dependence structures in the features \mathbf{X} . Our proposal, the marginal conditional expectation plot (MCEP), correctly considers these dependence structures and it provides convincing explainability results that reflect the empirical observations. Our third example concerns the **SH**apley **A**dditive **eX**planation (SHAP). We show that the neural network surrogate model for conditional expectations allows us to efficiently calculate the conditional SHAP decompositions both, for the mean but also for the decrease in deviance losses of the full model against the null model. The latter provides us with an interesting method for variable importance.

Acknowledgment. We kindly thank Michael Mayer for his methodological support and for supporting us in improving the figures.

References

- [1] Aas, K., Jullum, M., Løland, A. (2021). Explaining individual predictions when features are dependent: more accurate approximations to Shapley values. *Artificial Intelligence* **298**, article 103502.
- [2] Apley, D.W., Zhu, J. (2020). Visualizing the effects of predictor variables in black box supervised learning models. *Journal of the Royal Statistical Society, Series B* **82/4**, 1059-1086.
- [3] Brébisson, de A., Simon, É., Auvolet, A., Vincent, P., Bengio, Y. (2015). Artificial neural networks applied to taxi destination prediction. *arXiv:1508.00021*.
- [4] Breiman, L. (2001). Random forests. *Machine Learning* **45/1**, 5-32.
- [5] Carriere, J.F. (1996). Valuation of the early-exercise price for options using simulations and non-parametric regression. *Insurance: Mathematics & Economics* **19**, 19-30.
- [6] Charpentier, A. (2015). *Computational Actuarial Science with R*. CRC Press.
- [7] Cheridito, P., Ery, J., Wüthrich, M.V. (2020). Assessing asset-liability risk with neural networks. *Risks* **8/1**, article 16.
- [8] Delong, L., Kozak, A. (2023). The use of autoencoders for training neural networks with mixed categorical and numerical features. *ASTIN Bulletin* **53/2**, 213-232.
- [9] Dutang, C., Charpentier, A. (2018). CASdatasets R Package Vignette. Reference Manual. Version 1.0-8, packaged 2018-05-20.
- [10] Friedman, J.H. (2001). Greedy function approximation: a gradient boosting machine. *Annals of Statistics* **29/5**, 1189-1232.
- [11] Gneiting, T., Resin, J. (2022). Regression diagnostics meets forecast evaluation: Conditional calibration, reliability diagrams and coefficient of determination. *arXiv:2108.03210v3*.
- [12] Godin, F., Hamel, E., Gaillardetz, P., Ng, E.H.-M. (2023). Risk allocation through Shapley decompositions, with applications to variable annuities. *ASTIN Bulletin* **53/2**, 311-331.
- [13] Guo, C., Berkhahn, F. (2016). Entity embeddings of categorical variables. *arXiv:1604.06737*.
- [14] He, K., Chen, X., Xie, S., Li, Y., Dollár, P., Girshick, R. (2021). Masked autoencoders are scalable vision learners. *arXiv:2111.06377*.
- [15] Hiabu, M., Meyer, J.T., Wright, M.N. (2022). Unifying local and global model explanations by functional decomposition of low dimensional structures. *arXiv:2208.06151*.
- [16] Janzing, D., Minorics, L., Bloebaum, P. (2020). Feature relevance quantification in explainable AI: A causal problem. In: Chiappa, S., Calandra, R. (eds.), Proceedings of the Twenty Third International Conference on Artificial Intelligence and Statistics, *Proceedings of Machine Learning Research* **108**, 2907-2916.
- [17] Jonen, C., Meyhöfer, T., Nikolić, Z. (2023). Neural networks meet least squares Monte Carlo at internal model data. *European Actuarial Journal* **13/1**, 399-425.
- [18] Krah, A.-S., Nikolić, Z., Korn, R. (2020). Least-squares Monte Carlo for proxy modeling in life insurance: neural networks. *Risks* **8/4**, article 116.
- [19] Laberge, G., Pequignot, Y. (2022). Understanding interventional TreeSHAP: How and why it works. *arXiv:2209.15123*.
- [20] Lindholm, M., Lindskog, F., Palmquist, J. (2023). Local bias adjustment, duration-weighted probabilities, and automatic construction of tariff cells. *Scandinavian Actuarial Journal*, published online: 14 Feb 2023.

- [21] Lindholm, M., Richman, R., Tsanakas, A., Wüthrich, M.V. (2022). Discrimination-free insurance pricing. *ASTIN Bulletin* **52/2**, 55-89.
- [22] Longstaff, F., Schwartz, E. (2001). Valuing American options by simulation: A simple least-squares approach. *The Review of Financial Studies* **14**, 113-147.
- [23] Lundberg, S.M., Erion, G., Chen, H., DeGrave, A., Prutkin, J.M., Nair, B., Katz, R., Himmelfarb, J., Bansal, N., Lee, S.-I. (2020). From local explanations to global understanding with explainable AI for trees. *Nature Machine Intelligence* **2/1**, 2522-5839.
- [24] Lundberg, S.M., Lee, S.-I. (2017). A unified approach to interpreting model predictions. In: Guyon, I. Luxburg, U.V., Bengio, S., Wallach, H., Fergus, R. Vishwanathan, S., Garnett, R. (eds.), *Advances in Neural Information Processing Systems* **30**, 4765-4774.
- [25] Mayer, M., Meier, D., Wüthrich, M.V. (2023). SHAP for actuaries: explain any model. *SSRN Manuscript ID 4389797*.
- [26] Mayer, M., Stando A. (2023). SHAP visualizations. R package `shapviz`. Version 0.9.0.
- [27] Mayer, M., Watson, D., Biecek, P (2023). Kernel SHAP. R package `kernelshap`. Version 0.3.7.
- [28] McCullagh, P., Nelder, J.A. (1983). *Generalized Linear Models*. Chapman & Hall.
- [29] R Core Team. R: A language and environment for statistical computing. R Foundation for Statistical Computing. <http://www.R-project.org/>
- [30] Richman, R. (2021). AI in actuarial science - a review of recent advances - part 1. *Annals of Actuarial Science* **15/2**, 207-229.
- [31] Richman, R. (2021). AI in actuarial science - a review of recent advances - part 2. *Annals of Actuarial Science* **15/2**, 230-258.
- [32] Shapley, L.S. (1953). A value for n -person games. In: Kuhn, H.W., Tucker, A.W. (eds.), *Contributions to the Theory of Games*, AM-28, Volume II, Princeton University Press, 307-318.
- [33] Sundararajan, M., Najmi, A. (2019). The many Shapley values for model explanation. *arXiv:1908.08474*.
- [34] Tsai, C.P., Yeh, C.K., Ravikumar, P. (2022). Faith-Shap: The faithful Shapley interaction index. *arXiv:2203.00870*.
- [35] Tsitsiklis, J., Van Roy, B. (2001). Regression methods for pricing complex American-style options. *IEEE Transactions on Neural Networks* **12**, 694-703.
- [36] Wüthrich, M.V., Merz, M. (2023). *Statistical Foundations of Actuarial Learning and its Applications*. Springer Actuarial. <https://link.springer.com/book/10.1007/978-3-031-12409-9>
- [37] Zhao, Q., Hastie, T. (2021). Causal interpretations of black-box models. *Journal of Business & Economic Statistics* **39/1**, 272-281.